

Titan's surface reviewed: the nature of bright and dark terrain

Ralph D. Lorenz and Jonathan I. Lunine

Lunar and Planetary Laboratory, University of Arizona, Tucson, AZ 85721-0092, U.S.A.

Received 27 October 1996; revised 19 February 1997; accepted 28 March 1997

Abstract. A number of recent observational results concerning Titan's surface are synthesized in order to constrain possible surface physical states and compositions. With the remote sensing data as a guide, the surface is divided into two types of terrain, "bright" (extending from 60–160 deg Titan longitude) and "dark" (encompassing the rest of the object). Although substantial discrepancies exist in published near-infrared albedo estimates, which may be at least in part explained by Titan's aspect and seasonally-varying haze, the bright region has a surface albedo consistently 0.1 higher than the dark region. Red (673 nm) albedos of 0.45 and 0.35 are deduced for the bright and dark regions. Recently-revised radar data are reviewed, which show Titan to be very different from the Galilean satellites, in emissivity, backscatter cross section, and polarization. The data rule out "clean" water ice, and thick and widespread organic deposits. Titan's terrains exhibit radar properties resembling silicate-rich surfaces, with the "bright" terrain more "icy", but other surfaces are possible, and we note the likelihood of small-scale surface heterogeneity. Evidence for a bright north pole is also reviewed, and it is speculated that the poles may have more surface liquids than lower latitudes. Although remote sensing data sets will increase in quantity and quality over the coming five years, it is argued that a final resolution of the nature of Titan's surface must await the completion of the Cassini/Huygens mission, set to arrive at Saturn in 2004. © 1997 Elsevier Science Ltd

Introduction

The physical state and composition of Titan's surface constitutes an enduring puzzle in planetary science, stretching now over five decades of spectroscopic obser-

vation. The global layer of photochemically-produced haze has been a barrier to direct observation of the surface until very recently, when first Earth-based radar, and then near-infrared and optical observations at moderate spectral resolution began to sense the surface beneath the haze.

This is a review and synthesis paper which examines the suite of available remote sensing observations of Titan to arrive at a finite set of possible surface compositions and states. While the data do not admit a single solution with respect to the surface state, they do provide constraints and, perhaps more importantly, point to some potentially unusual properties of the surface of the solar system's second largest moon.

For the sake of brevity we do not attempt a comprehensive recitation of the literature on Titan's surface; Lorenz (1993), Lunine (1993), and Lunine and Lorenz (1996) and references therein should be consulted by the reader to provide appropriate background.

We consider Titan to be divided into two distinct regions, "bright" and "dark". These regions essentially correspond to Titan's leading hemisphere, known from infrared lightcurve monitoring (Lemmon *et al.*, 1993, 1995; Griffith, 1993; Coustenis *et al.*, 1995) to be brighter than the rest of Titan's surface. Maps made with the images from the Hubble Space Telescope (Smith *et al.*, 1996) show the outline of this discrete bright region, and indicate that other small regions are similarly bright.

For the purpose of this paper, we consider disk-averaged measurements with longitude of the central meridian (LCM) between 60 and 160°W to correspond to the bright terrain, with other values corresponding to "dark". Although the HST images indicate the "bright" region is limited between 10°N and 30°S—see Fig. 1—as most of the light in a disk-integrated measurement comes from the center of the disk, this longitudinal definition of bright terrain is reasonable.

Photochemically-based surface models

Because much of the remote sensing interpretation has been judged against a model of the surface based on

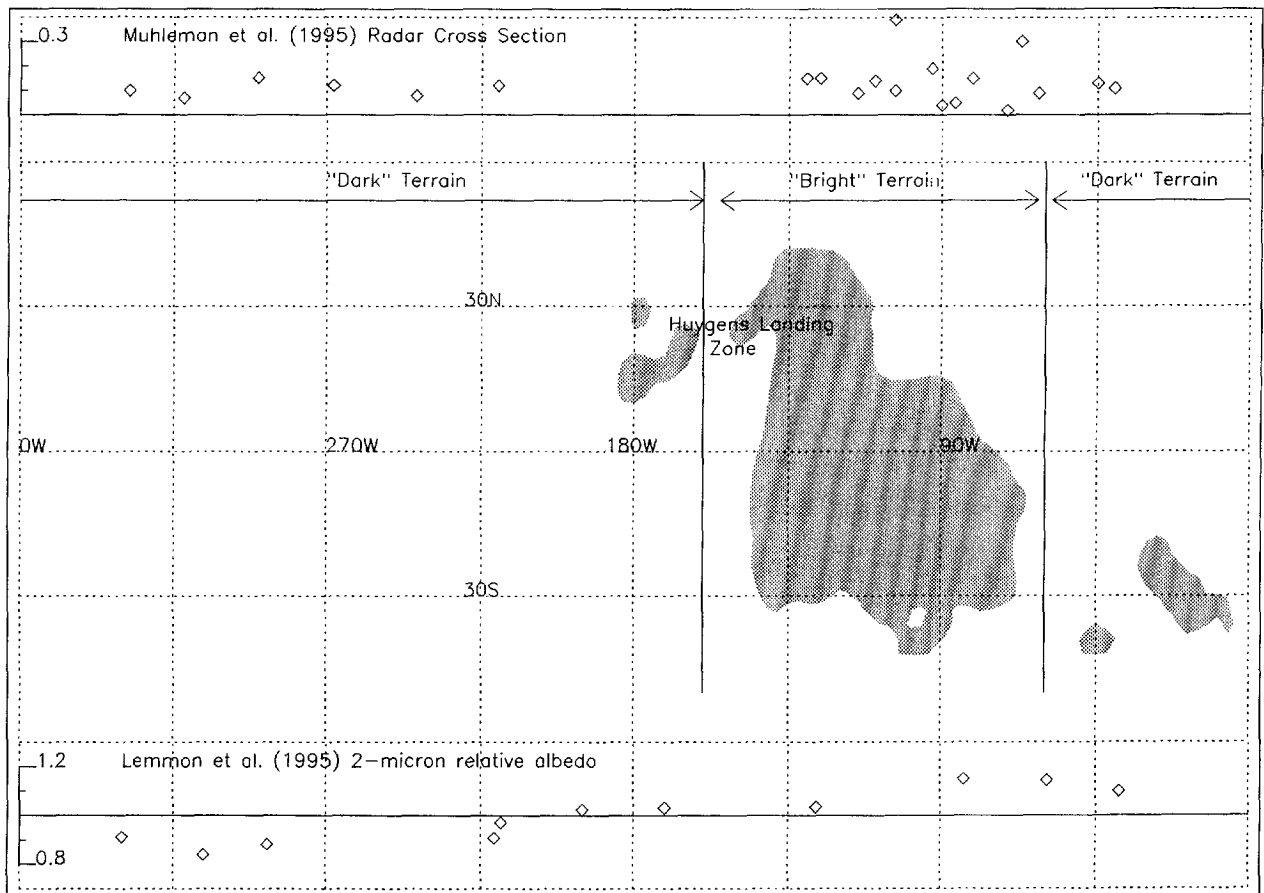


Fig. 1. Schematic map (cylindrical projection) of 940 nm surface reflectivity derived from F850LP data (Smith *et al.*, 1996). Longitudinal bounds on “Bright” and “Dark” terrains described in this paper are shown by vertical lines. Lemmon *et al.* (1995) 2 μ m relative albedo shown on the same longitude scale at bottom; opposite-sense (left-hand circular polarization) radar cross sections from Muhleman *et al.* (1995) shown at top, indicating higher reflectivities over the “bright terrain”. Approximate Huygens landing site is indicated

Voyager data and stratospheric methane photochemistry (Lunine *et al.*, 1983), we review this model here. Methane and photochemical byproducts have been detected from Earth for a half century, and the 1980 Voyager 1 flyby found the emissions to come from a stratosphere overlying a fairly thick troposphere, with a surface pressure of 1.5 bar at a temperature of roughly 95 K. The atmosphere is predominantly nitrogen, to the 98% level at the tropopause and perhaps 90% at the surface. The total amount of methane in the atmosphere, at the current rate of photolysis (which is irreversible because of rapid loss of hydrogen as a byproduct), would be depleted in a timescale of the order of 10^7 years (Yung *et al.*, 1984). This number has been confirmed by subsequent photochemical models (e.g. Lara *et al.*, 1994), as has ethane as the primary product of photosynthesis (with acetylene a close second).

Ethane, like methane, is liquid at the current surface temperature of Titan; mixtures of ethane, methane and nitrogen will have liquid phases down to significantly lower temperatures. Acetylene, on the other hand, is a solid at 95 K, with the tendency to explosively transform to polyacetylenes. Lunine *et al.* (1983) proposed a model in which methane was stored at the surface in liquid form, mixed with the products of its own photolysis (ethane and other liquid hydrocarbons), as well as with dissolved

nitrogen. The photochemical rate of Yung *et al.* (1984) implied 600–700 m of liquid ethane distributed globally on Titan's surface after 4.5 billion years of methane photolysis; an amount of liquid methane consistent with Voyager-derived atmospheric methane constraints led to a total liquid thickness of one to several kilometers (Dubouloz *et al.*, 1989); given topographic relief typically of cratered icy satellites, such a liquid layer would submerge much of the surface and lead to a global ocean.

Subsequently estimated ethane production rates (e.g. Lara *et al.*, 1994) were somewhat lower, implying perhaps 200 m of ethane and a total liquid layer some 0.5 km in thickness. The resulting fast currents in shallow seas were thought to be a problem for the tidal dissipation of Titan's orbital eccentricity (Sagan and Dermott, 1982; Sears, 1995). However, liquid dissipation may be reduced in crater basins (Dermott and Sagan, 1995). In any case the argument may be moot in the presence of significant interior dissipation (Sohl *et al.*, 1995)—dissipation in Titan's interior may be enough to make the high eccentricity difficult to explain, without invoking the additional complication of oceans.

Hence, a model consistent with the known photochemistry operating today on Titan, extrapolated over 4.5 billion years, leads to a liquid hydrocarbon surface layer

several hundred meters or more thick. Using Ganymede topography as a guide, such a layer would fill most crater basins but leave highlands exposed. Early remote sensing data from radar studies, which concluded a high surface reflectivity for Titan, suggested that even this much liquid was inadmissible. Models in which the liquid hydrocarbons are stored beneath the surface in a porous crust (Stevenson, 1992; Eluszkiewicz and Stevenson, 1990; Kossaki and Lorenz, 1996) have been advanced.

The baseline photochemical model, implying the possibility of substantial hydrocarbon liquids at the surface, motivated a suite of remote sensing observations in the visible, near-infrared, radio and via active radar experiments. We consider next the constraints on surface properties imposed by these various observations.

Near-infrared albedo

Griffith *et al.* (1991) made observations in windows between near-infrared methane absorption bands, and attempted to correct for atmospheric effects (haze, and methane absorption). The resultant albedos, they noted, were compatible with a mix of Ganymede and Phoebe, in the relative proportions of 1:2. This should be regarded simply as an example of a mixture of water ice and a dark material, which could be organic sediments, or hydrocarbon lakes.

Lemmon *et al.* (1993, 1995), observing Titan in the atmospheric windows noted that the albedo in the windows shows variations, and that these variations are correlated with orbital phase. This indicated that Titan's surface is heterogeneous, a result confirmed since by Griffith (1993) and Coustenis *et al.* (1995).

Noll and Knacke (1993) re-analyzed data by Cruikshank and Morgan taken in 1979 and showed that these data too exhibit a light curve. Additionally, they compared the $5\ \mu\text{m}$ albedo with the Galilean satellites, and noted that Titan resembled Callisto the most in this respect. (Callisto is the optically darkest of the Galileans, due to a higher mixing ratio of silicates on the surface. The silicates, however, make it brighter at $5\ \mu\text{m}$ than "cleaner" Ganymede.)

In 1992, Smith *et al.* obtained images of Titan using the Hubble Space Telescope. Among the filters used was one that sampled the methane window at 940 nm. This filter, however, also sampled the methane absorption band at 89 nm. By subtracting a separate 889 nm image, a residual image was left which it was believed indicated clouds or surface features. The images had to be processed considerably: this was prior to the repair of HST and the spherical aberration in the optics required that images be subjected to deconvolution, a process that is optimized for point sources. It is easy with Titan, an extended object with significant limb-brightening, to introduce artifacts, especially if the signal-to-noise of either the point-spread function or the image itself are poor. Thus, given deconvolution uncertainties and the inability to discriminate clouds from surface features (images were obtained at only one orbital phase) no confident conclusions could be drawn.

However, in 1994 Smith *et al.* obtained a set of images

covering almost the entire longitude range. This allowed the subtraction of a longitudinal average (a more reliable subtraction than the 889 nm band, since the limb-darkening in the F850LP filter covering the window differs from that in the FQCH4N-D filter which samples only the methane band). They also produced surface maps using the F673N and F1042M filter, covering the red continuum and the $1.07\ \mu\text{m}$ window (Smith *et al.*, 1996). The images used to make the maps were taken with the WFPC2, which corrected the spherical aberration. While deconvolution would in principle sharpen the images somewhat, to avoid introducing artifacts, the maps were made with raw (undeconvolved) images. The three maps agree closely with each other, and indicate a bright region (about $4000 \times 2500\ \text{km}$) near 110 W.

Ground-based near-infrared adaptive optics telescopes have been able to image Titan near $2\ \mu\text{m}$ (it is difficult to correct the wavefront distortions introduced by atmospheric turbulence much below this wavelength as the coherence lengths in the atmosphere become too short). An initial investigation by Saint-Pe *et al.* (1993) noted that Titan appears non-circular and may have bright regions. Like the 1992 HST results, however, lack of temporal or longitudinal coverage prevented conclusive identification of these regions as surface features. Subsequent observations have benefited from the rapid progress in adaptive optics: Han *et al.* (1995) and Combes *et al.* (1995) noted detection of the same feature at $2\ \mu\text{m}$ as shown at 0.94 and 1.07 in the HST maps. Combes *et al.* (1996, 1997) report that $2\ \mu\text{m}$ images resolve the bright region into three distinct centers of brightness, which is also consistent with, although less apparent in, the HST images (which have lower contrast; $\sim 10\%$ against $\sim 30\%$ at $2\ \mu\text{m}$).

Coustenis *et al.* (1995) compiled disk-integrated albedo data, and investigated the sensitivity of the observed albedo to surface reflectivity and methane absorption coefficient using the radiative code of McKay *et al.* (1989). They present consequent estimates for the maximum, minimum and average surface reflectivities at 1.07, 1.28, 1.58 and $2\ \mu\text{m}$, and compare the average values to the corresponding figures for Callisto and Ganymede. They suggest two spectrally distinct surface components are required, and that there is evidence of water ice absorption bands at all longitudes.

It should be noted that the correction for atmospheric effects is both substantial and non-linear. Inspection of Table 3 in Coustenis *et al.* (1995) shows that the inferred surface albedo for a given wavelength can be higher or lower than the observed value, and the correction depends strongly on wavelength. Lemmon *et al.* (1995) and Griffith *et al.* (1991) both use different models to infer surface albedos, so intercomparison is difficult. Even when, for example, the observed albedo used by Griffith *et al.* (1991) is converted to a surface value by interpolation from the corrections used by Coustenis *et al.* (1995), there are substantial discrepancies.

Combes *et al.* (1997) indicate that even the large dark region cannot be dominated by liquid methane and ethane, as these liquids absorb strongly at $2.1\ \mu\text{m}$ and would appear darker than observed. This interpretation, however, relies on the Coustenis *et al.* (1995) interpretation of absolute observed albedo, and the corresponding surface reflectivity.

Table 1. Visible and near-infrared albedo data

Wavelength	Titan (bright terrain)	Titan (dark terrain)	Europa ⁱ	Ganymede ⁱ	Callisto ⁱ	Hyperion ^h	Iapetus bright terrain ^h	Iapetus dark terrain ^h	Moon ^j (disk average)
673 nm	0.45 ^a	0.35 ^a	0.6	0.46	0.18	0.3	0.4	0.1	0.15
940 nm	0.47 ^b	0.37 ^b	0.6	0.46	0.19	0.35	0.4	0.13	0.1–0.2
1.07 μm	0.47 ^b 0.47 ^c	0.37 ^b 0.28 ^c	0.4	0.45	0.18	0.4	0.4	0.14	0.1–0.25
1.28 μm	0.37 ^b 0.58 ^c 0.12–0.18 ^d 0.4 ^e	0.27 ^b 0.45 ^c	0.45	0.35	0.18	0.4	0.35	0.14	0.25
1.58 μm	0.4 ^b 0.29 ^c 0.07–0.11 ^d 0.14 ^e	0.3 ^b 0.14 ^c	0.25	0.22	0.16	0.3	0.2	0.14	0.15–0.3
2.0 μm	>0.27 ^b 0.24 ^c 0.08–0.09 ^d 0.17 ^e	>0.07 ^b 0.17 ^c	0.09	0.15	0.1	0.18	0.1	0.14	0.3
5.0 μm	0.07 ^f 0.09 ^g		0.02 ^f	0.04 ^f	0.09 ^f				

^aOur estimate—see text.

^bLemmon *et al.* (1995).

^cCoustenis *et al.* (1995).

^dGriffith *et al.* (1991) (model interpretation of corrected data by Fink and Larson (1979).

^eOur estimate applying the Coustenis *et al.* (1995) model interpretation of Griffith *et al.*'s corrected Fink and Larson data

^fNoll and Knacke (1993).

^gNoll *et al.* (1996).

^hRelative reflectivities from Clark *et al.* (1986), scaled to fit albedos in Morrison *et al.* (1986).

ⁱClark and McCord (1980).

^jCruikshank (1968).

The albedo data (summarized in Table 1, and illustrated in Fig. 2) do not point unambiguously to any particular surface composition. Most authors refer to “dirty ice”. Certainly, compared with organic “tholin” material which has a normal Fresnel reflectivity of about 0.08–0.06 over the 0.5–10 μm range (Khare *et al.*, 1984), and Phoebe with an albedo of about 0.06 (Morrison *et al.*, 1986). Titan's surface is bright. It is also rather brighter than the Moon at short wavelengths. It does not, even over the bright region, appear to be as bright as Europa or Enceladus, however. Several other satellites, with variable ice/silicate proportions (and perhaps some organics) have spectra that are broadly similar to the Titan terrains.

Noll *et al.* (1996) point out weak evidence that the 5 μm lightcurve (Fig. 1d in Noll and Knacke (1993)) has a minimum close to the peak of the lightcurve at shorter wavelengths. This would be consistent with a Callisto-like composition of the dark regions and less silicate-rich composition for the bright terrain. However, the uncertainties on these data are large and a set of good longitudinally-resolved data covering both bright and dark terrain is required. Noll *et al.* (1996) also report, tentatively, that the continuum slope within the 5 μm band is incompatible with tholin's spectral shape.

Recently, Griffith *et al.* (1996) have identified another possible window through Titan's atmosphere, at 3 μm . As with the 5 μm window, albedo measurements over both

types of terrain would be useful constraints on their composition.

Visible albedo

While the revelations to date regarding the heterogeneity of Titan's surface have been made in the microwave and near-infrared, there in fact exists information on Titan's surface in the visible red part of the spectrum.

Smith *et al.* (1996) construct a map of part of Titan's surface using a narrow-band continuum filter at 673 nm (red). Both the map, and a longitudinal slice along the equator (their Fig. 4d), correlate strongly with those for the 940 and 1070 nm near-infrared windows. Thus, we know that those regions on Titan that are bright in the near-infrared are also bright in red. Comparing the height of the “saddle”, the characteristic double peak in the brightness against longitude curve, suggests the contrast between the bright and (unseen) dark side is about 50% of that seen in the longer wavelength filters, or about 5%.

McKay *et al.* (1989) (Fig. 6b) show the sensitivity of Titan's geometric albedo to the surface reflectivity as a function of wavelength. The sensitivity at red wavelengths is about half that in the near-infrared: red light is strongly scattered by the thick haze (as Smith *et al.* (1996) note, the normal incidence optical depth is of the order of 3—

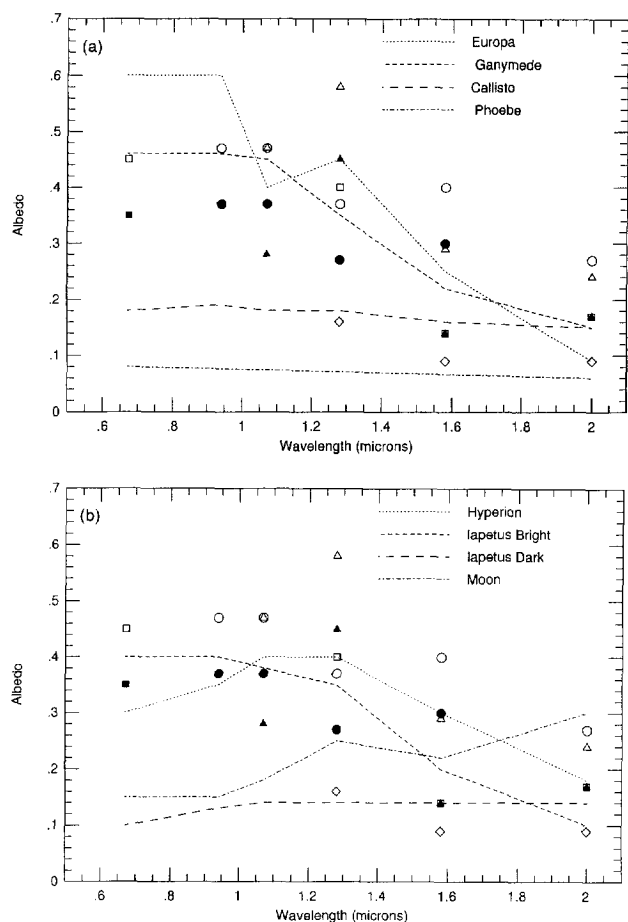


Fig. 2. (a) Red and near-IR surface albedos for Titan terrains, Phoebe and the Galilean satellites. Filled symbols correspond to dark terrain, open symbols to the bright region on Titan. Since there is substantial scatter in the Titan data, and published uncertainties may not be correct, error bars have not been included. Squares are the results of the present work, circles from Lemmon *et al.* (1995), triangles from Coustenis *et al.* (1995) and diamonds from Griffith *et al.* (1991). (b) As (a), but for Titan, Iapetus bright and dark terrain, Hyperion and the Moon

few photons reach the surface and return to the observer without encountering multiple scatterings in the atmosphere). McKay *et al.*'s geometric albedo (McKay *et al.*, 1989) at 640 nm increases by about 0.07 by varying the surface reflectivity from 0.0 to 0.2. Stammes (1992) presents models showing the albedo increasing by 0–0.18 for the same surface reflectivity change.

Hence, to a first order, at red wavelengths, the bright material has a reflectivity higher than the dark material by about 0.05–0.15. By comparison, the HST contrast is about 8% in the 1070 nm window, corresponding to an increment of about 0.18 in albedo (Coustenis *et al.*, 1995). McKay *et al.* (1989) predict an increase of 0.11 in observed albedo from surface reflectivities of 0.0–0.2. Thus, while somewhat indirect, and blurring the distinction between normal or near-normal brightness of a surface region and the disk-integrated albedo of the body as a whole, these comparisons make a strong argument that the surface reflectivity at red wavelengths is 0.1–0.2 brighter over bright regions than dark ones.

McKay *et al.* (1989) note that about half of the radiation reaching Titan's surface is below 700 nm in wavelength

(scattered) and half above 1000 nm (more or less direct). They use a surface reflectivity of 0.2 to reproduce Titan's surface temperature with a radiative–convective model, although values less than 0.4 can still give reasonable agreement with Titan's present atmosphere profile (Lorenz *et al.*, 1997). Since the reflectivity above 1000 nm determined by Coustenis *et al.* (1995), weighted by the relative contributions of surface insolation (McKay *et al.*, 1989, Fig. 11) is about 0.35, then it follows that the global average visible albedo must be 0.05–0.45. For the present, we assume “red” equivalent to “visible”, but note that in general the blue reflectivity of solar system materials is lower than the red values, so the “red” reflectivity of Titan is likely to be nearer the higher end of this range.

Knowing that this global visible albedo is a weighted sum of both bright (28%) and dark (72%) regions, and the difference of these is 0.05–0.15, it can be shown that the dark terrain must have a red reflectivity of 0–0.44 and the bright terrain 0.1–0.55.

Neff *et al.* (1984) report carefully-calibrated values of Titan's geometric albedo. The measurements were taken at Greatest Eastern Elongation, over the bright region on Titan's surface. A radiative transfer model by Lemmon (1994) shows best agreement with these data for a surface reflectivity of 0.45. For a 5% lower albedo (as over Titan's dark terrain) the reflectivity is 0.35. These estimates are reassuringly in the range indicated above, and not unsurprisingly at the higher end.

Use of a radiative transfer model directly on the HST images may yield more refined estimates of the visible albedo, though we are confident that such estimates will lie within our ranges above. Although this estimate does little to constrain Titan's surface composition at present, we note that it (or a revised value) may be of use in eliminating some surface candidates when near-infrared reflectivities are better known. For example, pyroxene is much brighter at 680 nm than at 940 nm, whereas plagioclase has a similar reflectivity at these two wavelengths.

Radar measurements of Titan's surface

We focus on the experiments of Muhleman and colleagues (Muhleman *et al.*, 1991, 1995) which are the only suite to have achieved useful signal-to-noise on Titan, the most distant object yet detected by radar. The Goldstone antenna was used as transmitter, with the Very Large Array (VLA) in Socorro in several configurations as receiver at 3.5 cm wavelength. The data can be divided radar cross section in two polarizations (same circular and opposite circular), and the spectral shape of the return. Additionally, measurements of Titan's thermal emission at 3.5 cm wavelength play an important interpretive role. Here we do not attempt to reproduce the detailed discussion of observations in Muhleman *et al.* (1995), but instead consider the implication of the radar data for the nature of Titan's surface.

We summarize radar data for Titan and a number of comparison objects in Table 2.

The original report of high (\sim)0.30 reflectivity in Muhleman *et al.* (1991), being the one and only observation of Titan's surface for some years, was a significant

Table 2. Microwave properties

Property	Titan (bright terrain)	Titan (dark terrain)	Europa	Ganymede	Callisto	Moon	Mercury	Venus
3.5 cm same sense (σ_{sc})	0.08 ± 0.08^a	0.03 ± 0.0^a	1.40 ± 0.23^b	0.9 ± 0.10^b	0.40 ± 0.04^b	0.006^k	0.005^e	0.06^e
3.5 cm opposite sense (σ_{oc})	0.16 ± 0.1^a 0.15 ± 0.05^c $0.35 \pm 0.08^{d,m}$ 0.15 ± 0.04^n	0.13 ± 0.03^a 0.10 ± 0.04^c	0.91 ± 0.13^b	0.65 ± 0.10^b	0.32 ± 0.02^b	0.07^i	0.06^e	0.13^e
Polarization ratio ($\mu_c = \sigma_{sc}/\sigma_{oc}$)	0.5^b $> 1?^n$	0.3^b	1.43 ± 0.23^b	1.40 ± 0.1^b	1.22 ± 0.08^b	0.1^b	0.1^k	0.5^k
Microwave emissivity	0.85^c	0.85^l	0.4^d	0.5^d	0.8^d	0.95^c		0.845^j
Radar limb coefficient	$1.5\text{--}3.0^e$	1.4^e	1.7 ± 0.4^b	1.3 ± 0.2^b	1.4 ± 0.3^b	1.5^f		

^aOur averages of $60^\circ < \text{LCM} < 160^\circ$ (bright region) and $\text{LCM} < 60^\circ$, $\text{LCM} > 160^\circ$ (dark region) data from Table 1 of Muhleman *et al.* (1995).

^bOstro *et al.* (1992).

^cMuhleman *et al.* (1995).

^dMuhleman *et al.* (1991).

^eOur own interpretation of Fig. 4 of Muhleman *et al.* (1991)—higher coefficients give better fits to the averaged data.

^fPettengill (1965).

^gGoldstein and Green (1980).

^hFrom our data.⁴

ⁱMuhleman *et al.* (1995) report measuring $\sigma_{sc} > \sigma_{oc}$ on two occasions, both over “bright” longitudes.

^jAverage Magellan value from Ford *et al.* (1993). Values range from 0.35 to 0.95.

^kFrom data in table, from (Venus, Mercury)^g and (Moon).^{b,i}

^lGrossman and Muhleman (1992) suggest minimal emissivity lightcurve, so dark value = bright value.

^mMuhleman *et al.* (1991) report the cross section of Titan at 0.75 ± 0.15 on June 4, 1989, whereas the cross section for the same observation, reported in Muhleman *et al.* (1995) is given as 0.35 ± 0.05 . Similarly, the averaged cross sections for June 3 + 4 + 5, 1989, are reported as 0.35 ± 0.08 and 0.15 ± 0.03 , respectively, although the authors do not mention this discrepancy, which is described in the text of the present paper.

ⁿGoldstein and Jurgens (1992).

driver of theoretical work on Titan's surface, notably prompting attempts to reconcile this high reflectivity with surface models that provided a methane reservoir. The subsequently-published summary (Muhleman *et al.*, 1995) gives a value of 0.15 for this same bright region. An erroneous factor of 2 was introduced in the earlier reported results.

Goldstein and Jurgens (1992) used the Goldstone radar antenna in a monostatic mode (i.e. Goldstone was both transmitter and receiver). Adding five days of observations—this highlights the challenging nature of these observations—yielded a cross section of 0.14 ± 0.03 , consistent with the revised values from the VLA.

As before, the radar reflectivity of Titan can be roughly divided into “brighter” and “darker” signatures. We find, using data tabulated in Muhleman *et al.* (1995), that the mean values of backscatter cross section for the bright longitudes are higher than for the dark terrain (at both polarizations), but with marginal statistical significance (a significance test indicates that the bright terrain is brighter with a standard variate of a little over 1.0, whereas a value of 2.0 is required for 95% confidence).

The brighter terrain possesses reflectivities inconsistent with the signature from a hydrocarbon ocean, even one which might be foamy or contain near surface particulates (the problem of floating solids of higher density in the low-density hydrocarbon ocean model is discussed in Lunine (1992)). The reflectivity of the darker terrain is also inconsistent with the presence of liquid hydrocarbons, but not by much. In fact, much of the early discussion surrounding the radar data as mitigating against widespread liquid

hydrocarbons took place after the initial observations (Muhleman *et al.*, 1991), which tended to yield a higher cross section than the overall body of the radar data available today (see Table 2 and footnotes thereto). Titan is more radar-reflective than a body covered completely by a hydrocarbon ocean or tholin but is still a low-reflectivity body when the bright area is distinguished from the remainder of the object. As far as the radar data are concerned, solid and even liquid hydrocarbons could indeed cover a fair fraction of the darker terrain.

With respect to the bright terrain, the high originally-reported peak reflectivity was consistent with values for Ganymede and Callisto. These reflectivities, particularly the very high values from Europa, and the unusual tendency for the same-sense polarization to dominate from the Galilean satellites, are generally considered to be a signature of water ice (and have been used to infer the presence of ice at the poles of Mercury (Butler *et al.*, 1993) and the Moon (Nozette *et al.*, 1996). Various mechanisms have been invoked to explain the polarization, for example refraction in ice density gradients, reflection from craters acting as retroreflectors, and coherent scattering from inhomogeneities in ice. Ostro and Shoemaker (1990) consider these mechanisms in terms of their geological plausibility and note that high-order multiple scattering is likely to be responsible for the high backscatter coefficients. The various mechanisms are summarized with discussion in Butrica (1996).

The revised reflectivity is considerably smaller than even that from Callisto, and seems (see Fig. 3) more like the rocky surfaces of the inner solar system. This is at odds

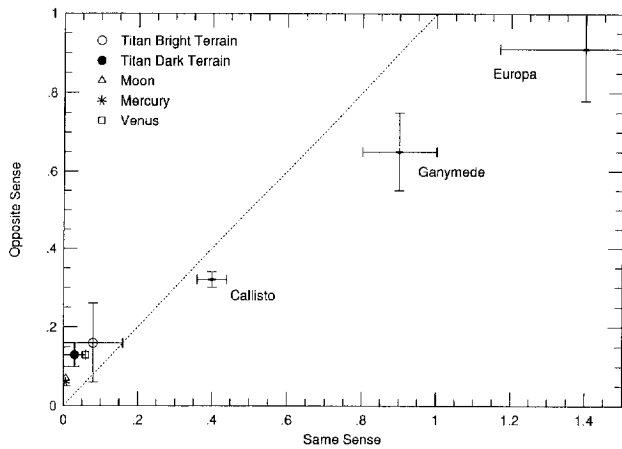


Fig. 3. Radar cross sections in the same and opposite circular polarizations of various solar system bodies. The icy Galilean satellites lie to the right of the dashed line which indicates unity polarization ratio. Rocky terrestrial planets have small cross sections, and lie to the left of the line, as do both Titan terrains (although the bright terrain's error bars cross into the "icy" region)

with the very icy appearance at infrared wavelengths. We therefore seek additional information in the other radar parameters, namely polarization and Doppler shape.

Same-sense polarization dominated from Titan on only two nights of observation, one of which involved a high cross section but the other yielded only an average cross section. Other nights with large returns had opposite-sense polarization dominating. Thus, while it is tempting to associate the same-sense return as being a signature of clean water ice, the association of high return with same-sense return does not apply consistently to Titan as it does to the Galilean satellites. Therefore, caution must be applied in ascribing the high returns to clean water ice, though this remains the favored explanation. Perhaps the physical structure of the ice, or presence of compounds such as ammonia hydrates in the ice, alter the return enough to defeat mechanisms responsible for same-sense polarization. We concur with Muhleman *et al.*'s assessment that the same-sense polarization data are "mysterious", but we point out that the presence of opposite-sense polarization in some of the higher cross-section data is also a complication for any interpretation involving pure water ice. Figure 2 shows the radar cross sections for the two polarizations for a number of bodies—Titan is clearly different from the Galilean satellites.

Muhleman *et al.* (1995) report that the Doppler spectral shape of Titan is well-represented by a $\cos^n \phi$ where ϕ is the angle of incidence and n is a scattering law exponent, with $n = 1.4$ for Titan. By comparison, Ostro *et al.* (1992) report values of n of 1.7, 1.3 and 1.4 for Europa, Ganymede and Callisto at the same wavelength (3.5 cm) with an r.m.s. dispersion of 0.4, 0.2 and 0.3, respectively. As before, Titan seems to resemble Callisto most closely. Muhleman *et al.*'s spectral shape (Muhleman *et al.*, 1995) is based on an average of seven nights of data, of which only one samples the "bright" longitude, so to a first order, this figure may be taken as representative of "dark" terrain. Muhleman *et al.* (1991) present fits for their 1989 data, which sample only the bright terrain, and exam-

ination of their Fig. 4 suggests that the bright terrain has a rather higher exponent, perhaps 2–3.

A higher exponent indicates a more specular reflection, corresponding to either a topographically smoother surface, one where the poles are bright compared to the equator (the Doppler shape relies on the relative velocities of points on the surface, which are maximized at the equator: in a Doppler sense, the poles are in the same spectral location as the sub-telescope point) or perhaps where there is a strong backscatter gain (due to high-order reflections in ice).

Finally, comparison of the cross section versus emissivity reveals that Titan, much more than the Galilean satellites, obeys Kirchhoff's law in the sense that the cross section and emissivity add to unity. Interestingly, this plot (Fig. 4) has been used previously to argue that Titan "most" resembles Callisto (Muhleman *et al.*, 1995). However, Titan is more like the Earth's moon in terms of both absolute cross section and emissivity, and considering the dark terrain alone makes this point even more dramatically. This does not mean that the surface of the dark terrain on Titan is necessarily dominated by material compositionally and texturally like lunar-type silicates. Instead, it points out the hazards of using a small set of parameters to compare one body against another. Titan is a unique object in terms of its radar cross section, polarization behavior, and emissivity. The connection of these properties to an actual surface composition is a non-unique exercise. Perhaps the radar have been most valuable in discovering the heterogeneity of the surface, confirmed by infrared imaging, which bodes well for interesting results from the Cassini/Huygens mission (discussed further below).

Latitudinal and temporal variations

The maps of Titan published by Smith *et al.* (1996) do not necessarily indicate the absolute reflectivity of different regions on Titan, in that the subtraction of a longitudinal average effectively removes any latitudinal trends. In any

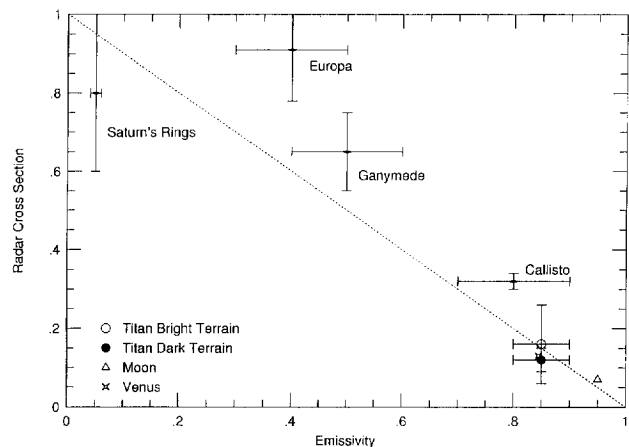


Fig. 4. Radar cross sections (opposite-sense) against microwave emissivity. Again, both Titan terrains resemble rocky (silicate) surfaces. The dashed line corresponds to Kirchhoff's law (emissivity = 1 - reflectivity) which applies in the absence of backscatter directivity, seen in the anomalously high cross sections for the Galilean satellites

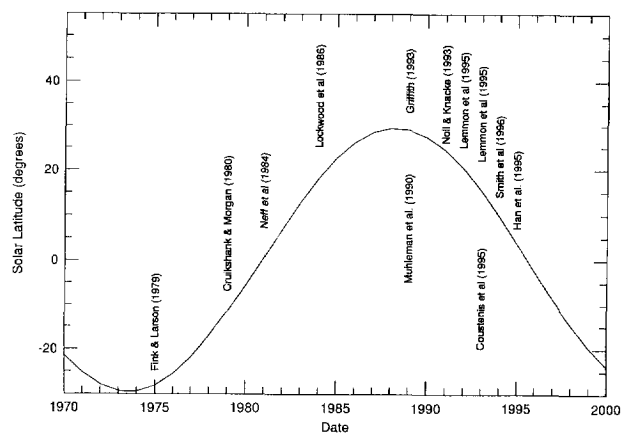


Fig. 5. The subsolar latitude on Titan, corresponding (within 3 deg) to the subtelescope latitude, during different observations. Where observations span several years, the best-covered year is indicated. The large span of latitudes covered may, in part, explain the substantial discrepancies between measurements

case, since the haze opacities in the two hemispheres are different (Lorenz *et al.*, 1997), extracting the true surface reflectance at different latitudes would be a difficult exercise.

Combes *et al.* (1996) report that infrared adaptive optics images at $2\ \mu\text{m}$ show that high northern latitudes are uniformly brighter than equatorial or southern latitudes. This could be an artifact (due to different haze contributions in the window-center and window-edge images which are differenced to produce the surface image, as performed by Smith *et al.* for the 1992 HST images), enhanced cloudiness over the polar regions (as on Earth), or a surface brightness. Combes *et al.* (1996) report also a slight brightening at high south latitudes.

Noll and Knacke (1993) report that their measurements in 1991 of the albedo in the $1.1\ \mu\text{m}$ window were consistently 14% higher than those recorded in 1979 by Cruikshank and Morgan (1980) at the same longitudes.

In 1991, the sub-Earth latitude on Titan was about 20°N , while in 1979 it was near-equatorial. A seasonal effect, or bright polar regions (either due to clouds or bright surface material) could be responsible. The variation in aspect of Titan is illustrated in Fig. 5—different observers are clearly looking at different parts of Titan.

Karkoschka (1994) compares his spectra of Titan and outer planets with those of Neff *et al.* (1984), Lockwood *et al.* (1986) and Fink and Larson (1979). His data, taken in 1993, agree (to approximately the noise level) with those of Lockwood *et al.* (1986), although Lockwood *et al.*'s data does not extend into the window regions longward of $900\ \text{nm}$. Karkoschka's spectrum (Karkoschka, 1994) in the $940\text{--}1000\ \text{nm}$ region has a shape much more consistent with that of Lemmon *et al.* (1993) and Fink and Larson (1979) than with Neff *et al.* (1984). This is surprising, given that the Lemmon and Karkoschka data were taken at the same latitude as Neff *et al.* (see Fig. 5). Karkoschka (1994) notes that there are discontinuities in the Neff albedo spectrum, and that a slope (due apparently to a relatively blue spectrum assumed for the sun) is present that makes Titan redder than it should be (see Fig. 4 in Karkoschka

(1994)). Thus, the Neff *et al.* (1984) data set is probably no longer the best to use to constrain models.

Lorenz *et al.* (1997) compare disk-integrated photometry of Titan with HST observations of the north-south asymmetry in Titan's atmosphere, which is a seasonal effect of haze at about $100\ \text{km}$ altitude. The peak blue contrast is about 18%, and corresponds to a brightening of about 5%. The disk-integrated albedo increase is due in part to the brighter (summer) hemisphere being tilted towards the observer, and in part to an overall brightening. The corresponding asymmetry at $1.07\ \mu\text{m}$ is 20%, in the opposite sense (the haze is dark in visible, and bright in the near-infrared). Thus, while the blue albedo increased by about 4% between 1979 and 1991, the near-infrared albedo should have decreased over that period, if the haze were responsible. Thus it seems reasonable to conclude that the discrepancy noted by Noll and Knacke (1993), and apparent in Combes *et al.*'s imaging results, indicates a real brightness either low in the atmosphere or on the surface.

It is of note that all the detections of radar reflectivity above 0.15 occurred in 1989–1991; subsequent detections have all been lower than this value. This would be consistent with a radar-bright north polar region contributing less and less to the disk-integrated value. The radar reflectivity of even thick methane clouds would be minimal. Smith *et al.* (1996) hypothesized that the bright feature in the HST images may be due to washing of highland terrain by methane rainfall (i.e. removing dark organics and exposing bright ice bedrock); it is possible that polar regions may be similarly washed.

Stevenson and Potter (1986) considered the implications of a drop in temperature of several degrees from Titan's equator to its pole, motivated by Voyager IRIS data that are consistent with (but do not require) such a gradient. They found that $\text{CH}_4\text{--N}_2$ saturation would occur all the way to the surface at polar latitudes, creating a liquid $\text{CH}_4\text{--N}_2$ cap. Seasonal transport of vapor from one cap to the other would pin the polar temperatures at identical values.

Such a cap, if it were solid, would provide a simple mechanism for creating a frosty north pole bright at near-infrared and radar wavelengths. However, Voyager IRIS data do not allow temperatures lower than the $\text{CH}_4\text{--N}_2$ solidus (or even below the pure CH_4 freezing point). A liquid cap, while thermodynamically allowable, does not seem to fit the remote sensing constraints—it would appear dark. The apparent absence of a liquid cap in the remote sensing data leaves us with the situation described above: a pole more humid than the equator, possibly cooler than it (although more recent IRIS data reductions (McKay *et al.*, 1989) suggest the equator-to-pole brightness gradient attributed by Stevenson and Potter (1986) to surface temperature is instead due to stratospheric emission), allows rainfall to reach the surface with sufficient frequency to wash away dark organics and expose clean ice beneath.

An alternative scenario has been advanced by Samuelson *et al.* (1996) who have suggested that IRIS data indicate that the mole fraction of methane decreases with latitude—unless this were accompanied by a drop in temperature, the methane humidity is lower at high latitudes than near the equator. This, they argue, is because a strong

seasonal effect (high latitudes being in darkness for several years in winter) promotes condensation of C_4N_2 , which in turn acts as nucleation centers for ethane condensation. Thus the ethane flux at high latitudes is higher, and as surface liquids are enriched in ethane, the methane humidity (in equilibrium with the ethane–methane liquids on the surface, with ethane-rich mixtures having lower equilibrium methane humidities) is lower.

The rather divergent interpretations of data from the same instrument highlight the need for more data. However, both of these scenarios suggest many lakes and seas at high latitude—since these are near the limb as viewed from Earth and therefore viewed at lower elevation, the remote sensing signature would be one of the solid surface (e.g. the crater walls that define the lake-shore), rather than that of the liquid. A large-scale liquid polar cap also suffers the problem that there is nothing to confine it to high latitudes: what may be thermodynamically the equivalent of a liquid polar cap is instead more likely to be manifested geomorphologically as isolated lakes, and rivers flowing to lower, less humid latitudes, where they evaporate. Both scenarios also imply higher precipitation fluxes (of one type or another) in polar regions.

Future ground-based and Cassini studies

The discrepancies identified in this review highlight the difficulties in both making and interpreting observations of an object that is small, remote and shows both spatial and temporal variations. Clearly better data is needed.

The near-infrared albedo is the subject of intense ongoing work, both in making observations (especially spatially-resolved ones), and in interpreting spectral data. The increasing availability of large telescopes and more sensitive detectors on the ground hold promise for progressively more sensitive visible and near-infrared measurements of Titan. Adaptive optics techniques will ensure spatial resolutions approaching those of Hubble Space Telescope, but NICMOS images of Titan from HST may still provide the best near-infrared information—observations of Titan with this instrument are planned in the autumn of 1997. The paucity of longitudinally-resolved $5\ \mu\text{m}$ albedo information is frustrating: a more reliable anticorrelation of $5\ \mu\text{m}$ albedo with shorter wavelengths would be useful in pointing to silicates as the principal darkening agent. Reduction and interpretation of image data is non-trivial, since the atmosphere makes a significant contribution to the received light. Further complications and artifacts can be introduced by the deconvolution that is required for ground-based measurements.

Interpretation of spectral data (and the full exploitation of imaging data) rely on the improvement of atmosphere models with appropriate methane absorption coefficients. It is probable that a single global atmosphere (haze) model will not be adequate for this task, given the considerable variation of haze opacity with latitude and time (Lorenz *et al.*, 1997). In other words, the haze models used in image reduction to date have been tuned to fit global

average albedo values, but since the haze structure has substantial latitudinal variation then these haze models may not actually describe the haze structure at any one point. Further, even if a haze model is a reasonable description of the global average haze structure, the latitudinal variations imply that the local opacity will depart significantly from a global average. Thus much more sophisticated, two-dimensional, models will be needed for confident estimation of absolute reflectivities over the surface.

Future radar observations (at both 3.5 cm and other wavelengths) are essential to interpreting the existing radar data sets. Note that a failure to measure the same high radar brightnesses seen by Muhleman *et al.* (1991) would not necessarily imply these earlier measurements were in error: a bright north pole which could have contributed to the high radar albedo in 1989–1991 will not be visible again from Earth until after 2010. Radar observations of Iapetus, marginally possible from Earth and perhaps feasible from Cassini, would be extremely valuable in comparing the surfaces of Titan and Iapetus, since the IR/visible surface spectrum of Iapetus is not obscured by an atmosphere.

Both the Cassini orbiter radar and the probe radar altimeter operate at Ku band, with about 3 cm wavelength, similar to the wavelength probed by Muhleman's experiments. These investigations will resolve issues of surface heterogeneities at scales of 100 m or higher. However, they will probably not tell us a great deal more about the subsurface structure, unless pure patches of low-absorption-coefficient material are found on that spatial scale.

Imagery of Titan's surface from the Cassini Orbiter VIMS and ISS instruments appears feasible. While the former is more likely to penetrate the methane and the haze, the latter has the higher spatial resolution. The ability of ISS to get interpretable, high signal-to-noise images will depend on careful selection of encounter geometries (near-nadir imaging is likely to be required to see the surface, so as to minimize the optical path length through the thick hazy atmosphere), as well as of filters. Matching the filter bandpass to the width of the window maximizes the observed contrast. Additionally it is planned to use cross-polarization filters: these will minimize the contribution of light scattered by the haze, just as reflections on water can be eliminated by polarizing glasses to aid fishing.

Schmitt *et al.* (1992) note the infrared spectra of hydrocarbon mixtures, and show that it may be possible to discriminate between possible surface mixtures using the spectrometer on the DISR instrument on the Huygens Probe. They demonstrated that with the spectral resolution of DISR, it will be possible to distinguish between, for example, ethane-rich and methane-rich mixtures.

Lorenz and Lunine (1995) compared the tradeoffs of spatial coverage and resolution for Cassini Orbiter and Huygens Probe experiments; in general the mission has enormous capability over a wide range of wavelengths to cover the surface of Titan at hundred meter scales, selected areas at tens of meters, and the probe landing site down to tens of centimeters resolution. The ability of the mission to examine a significant fraction of the surface of Titan at hundred meter to kilometer scales depends on the final

tour design which has yet to be selected. Provided the selected Cassini tour is capable of yielding such coverage, further ground-based studies will become most useful in examining temporal changes.

Conclusion: what is the nature of Titan's surface

In interpreting remote sensing data, particularly the radar where the information content lies in a small number of parameters such as radar cross section at one or two wavelengths, extreme care must be taken in comparing Titan to other natural solar system surfaces. The fact that Titan's radar cross section "most" resembles Callisto's out of a small suite of similarly-sized bodies does not mean that the physical state and composition of the surface is similar to that of Callisto. The non-uniqueness of the radar signature, particularly for the dark component, must be borne in mind. A number of different materials might yield the same radar signature, and the problem of mixing at sub-resolution spatial scales makes interpretation all the more difficult.

To date, the infrared data is sorely hampered by calibration uncertainties and the (model-dependent) removal of atmospheric effects. Apart from the suggestion of water ice absorption, and the incompatibility with a totally-organic covered surface, the IR data do not tightly constrain the surface composition. Indeed, depending on which data set is used, Titan has been compared with Ganymede, a Ganymede-Phoebe mix, Callisto and Hyperion. The surface is clearly not like the Moon or Phoebe alone, however, some brightening material is needed.

Titan's radar signature, however, is not at all like Callisto's, nor of Europa nor Ganymede. In particular, the polarization behavior of the reflected signal is unusual when compared with other solar system bodies, and is not well understood. Although Titan is similar in density and size to Ganymede and Callisto, its thick atmosphere distinguishes it from the giant moons of Jupiter. The atmospheres of all other solar system bodies (including, probably, that of Venus) interact with surface and subsurface reservoirs of volatiles on timescales much less than the age of the solar system. Titan's surface should show the effects of eons of methane photolysis, in the form of organic deposits of various kinds, whether or not source reservoirs of liquid methane (mixed with other hydrocarbons) are exposed or buried. The difficulty in identifying such deposits is a symptom of the challenge to remote sensing observation to penetrate the thick atmosphere (near-infrared), provide sufficient signal-to-noise (radar), or to obtain sufficient spatial resolution from a billion miles away (all techniques).

With the data at hand, it is not possible to produce a unique description of the surface of Titan. It is tempting from both the radar and infrared data to identify the surface composition as dominated by silicates and ice, with the bright terrain being somewhat icier, but such an interpretation is not the only one consistent with the available data. The density and thermal history of Titan (Lunine and Stevenson, 1987) is such that a silicate-rich crust is unlikely to be primordial—if the surface is indeed

largely covered in silicates, this would point strongly to a resurfacing event, probably in the wake of the break-up of proto-Hyperion (Farinella *et al.*, 1990)—due to the orbital resonance between Hyperion and Titan, the debris from the impact that destroyed proto-Hyperion fell mostly on Titan, adding perhaps several kilometers of material to the surface. Organic materials almost certainly modify the surface signature, but how and to what extent is still impossible to determine.

What is clear is that when all the data (both IR and radar) are considered together, Titan's surface is like nowhere else yet observed in the solar system.

Finally, it must be remembered that the surface assuredly is heterogeneous on scales much less than the currently-available spatial resolution from all remote sensing techniques—our division into bright and dark terrain is only the first step in dividing Titan into different regions, and we have already pointed to the possibility of polar terrains being rather different ("wetter") than lower latitudes. Like all bodies explored to date in the solar system, spacecraft observations using multiple techniques at very high spatial resolution will be needed to reveal the true nature of Titan's surface. The Cassini/Huygens mission is, for this reason, awaited eagerly.

Acknowledgements. The authors acknowledge the support of the Cassini project in the preparation of this work. Some of the research described herein was supported also by the NASA Research and Analysis Program. R.D.L. thanks Mark Lemmon for access to his radiative transfer model, and acknowledges informative discussions with Byron Han regarding deconvolution of adaptive optics images and Bryan Butler for explaining the discrepancy between reported values of radar reflectivity.

References

- Butler, B. J., Muhleman, D. O. and Slade, M. A. (1993) Mercury: full-disk radar images and the detection and stability of ice at the north pole. *J. Geophys. Res.* **98**, 15003–15023
- Butrica, A. J. (1996) *To See the Unseen—A History of Planetary Radar Astronomy*, NASA SP-4218.
- Clark, R. N. and McCord, T. B. (1980) The Galilean satellites: new near-infrared reflectance measurements (0.65–2.5 microns) and a 0.325–5 micron summary. *Icarus* **41**, 323–339.
- Clark, R. N., Fanale, F. P. and Gaffey, M. J. (1986) Surface composition of satellites. In *Satellites*, eds J. A. Burns and M. S. Matthews. University of Arizona Press, Tucson, 437–491.
- Combes, M., Vapillon, L., Gendron, E., Coustenis, A. and Lai, O. (1995) Spatially resolved images of Titan in the near-infrared. *Bull. Am. Astron. Soc.* **27**, 1106.
- Combes, M., Coustenis, A., Vapillon, L., Gendron, E., Wittemberg, R. and Sirdey, R. (1996) Images of Titan's surface in the near-IR with ADONIS. *Bull. Am. Astron. Soc.* **28**, 1130.
- Combes, M., Vapillon, L., Gendron, E., Coustenis, A., Lai, O., Wittemberg, R. and Sirdey, R. (1997) Spatially-resolved images of Titan by means of adaptive optics. *Icarus* (submitted).
- Coustenis, A., Lellouch, E., Maillard, J. P. and McKay, C. P.

- (1995) Titan's surface: composition and variability from the near infrared albedo. *Icarus* **118**, 87–104.
- Cruikshank, D. P. (1968) Infrared colorimetry of the Moon. Ph.D. Dissertation, University of Arizona.
- Cruikshank, D. P. and Morgan, J. S. (1980) Titan: suspected near-infrared variability. *Astrophys. J.* **235**, L53–L54.
- Dermott, S. F. and Sagan, C. (1995) Tidal effects of disconnected hydrocarbon seas on Titan. *Nature* **374**, 238–240.
- Dubouloz, N., Raulin, F., Lellouch, E. and Gautier, D. (1989) Titan's hypothesized ocean properties: the influence of surface temperature and atmospheric composition uncertainties. *Icarus* **82**, 81–96.
- Eluszkiewicz, J. and Stevenson, D. J. (1990) Physico-chemical state of Titan's subsurface layers. *Lunar and Planetary Science Conference XXI (abstracts)*, pp. 323–324.
- Farinella, P., Paolicchi, P., Strom, R. G., Kargel, J. S. and Zappala, V. (1990) The fate of Hyperion's fragments. *Icarus* **83**, 186–204.
- Fink, U. and Larson, H. P. (1979) The infrared spectra of Uranus, Neptune, and Titan from 0.8 to 2.5 microns. *Astrophys. J.* **233**, 1021–1040.
- Ford, J. P. *et al.* (1993) Guide to Magellan image interpretation. JPL Publication 93-24.
- Goldstein, R. M. and Green, R. R. (1980) Ganymede: Radar surface characteristics. *Science* **207**, 179–180.
- Goldstein, R. M. and Jurgens, R. F. (1992) DSN observations of Titan TDA PR 42-109. Jet Propulsion Laboratory.
- Griffith, C. A. (1993) Evidence for surface heterogeneity on Titan. *Nature* **364**, 511–514.
- Griffith, C. A., Owen, T. and Wagener, R. (1991) Titan's surface and troposphere, investigated with ground-based near-infrared observations. *Icarus* **93**, 362–378.
- Griffith, C. A., Miller, G., Owen, T., Han, B., McKay, C. and Geballe, T. (1996) Titan: a study of the lower atmosphere and surface. *Bull. Am. Astron. Soc.* **28**, 1130.
- Grossman, A. W. and Muhleman, D. O. (1992) Observations of Titan's radio light-curve at 3.5 cm. (abstract). *Bull. Amer. Astron. Soc.* **24**(3) 954.
- Han, B., Owen, T., Brahic, A., Dumas, C., Roddier, F., Roddier, C., Northcott, M., Graves, J. E. and O'Connor, D. (1995) Ground-based near-infrared adaptive-optics imaging of the surface of Titan. *Bull. Am. Astron. Soc.* **27**, 1104.
- Karkoschka, E. (1994) Spectrophotometry of the Jovian planets and Titan at 300 to 1000 nm wavelength: the methane spectrum. *Icarus* **111**, 174–192.
- Khare, B. N., Sagan, C., Arakawa, E. T., Suits, F., Callcott, T. A. and Williams, M. W. (1984) Optical constants of organic tholins produced in a simulated Titanian atmosphere: from soft X-ray to microwave frequencies. *Icarus* **60**, 127–137.
- Kossaki, K. J. and Lorenz, R. D. (1996) Hiding Titan's ocean: densification and hydrocarbon storage in an icy regolith. *Planet. Space Sci.* **44**, 1029–1037.
- Lara, L. M., Lorenz, R. D. and Rodrigo, R. (1994) Liquids and solids on the surface of Titan: results of a new photochemical model. *Planet. Space Sci.* **41**, 5–14.
- Lemmon, M. T. (1994) Properties of Titan's Haze and Surface. Ph.D. Thesis, University of Arizona.
- Lemmon, M. T., Karkoschka, E. and Tomasko, M. (1993) Titan's rotation: surface feature observed. *Icarus* **103**, 329–332.
- Lemmon, M. T., Karkoschka, E. and Tomasko, M. (1995) Titan's rotational lightcurve. *Icarus* **113**, 27–38.
- Lockwood, G. W., Lutz, B. L., Thompson, D. T. and Bus, E. S. (1986) The albedo of Titan. *Astrophys. J.* **303**, 511–520.
- Lorenz, R. D. (1993) The surface of Titan in the context of ESA's Huygens Probe. *ESA J.* **17**, 275–292.
- Lorenz, R. D. and Lunine, J. I. (1995) Erosion on Titan. *Icarus* **122**, 79–91.
- Lorenz, R. D., Smith, P. H., Lemmon, M. T., Karkoschka, E., Caldwell, J. and Lockwood, G. W. (1997) Titan's north-south asymmetry from HST and Voyager imaging: comparison with models and groundbased photometry. *Icarus* **127**, 173–189.
- Lunine, J. I. (1992) Plausible surface models for Titan. *Symposium on Titan*, ESA SP-338, pp. 17–22.
- Lunine, J. I. (1993) Does Titan have an ocean? A review of current understanding of Titan's surface. *Rev. Geophys.* **31**, 131–149.
- Lunine, J. I. and Lorenz, R. D. (1996) The surface of Titan revealed by Cassini/Huygens. *Proceedings of SPIE—International Society for Optical Engineering*, Denver, Colorado, August 1996. Vol. 2803, pp. 45–54.
- Lunine, J. I. and Stevenson, D. L. (1987) Clathrate and ammonia hydrates at high pressure: application to the origin of methane on Titan. *Icarus* **70**, 61–77.
- Lunine, J. I., Stevenson, D. J. and Yung, Y. L. (1983) Ethane ocean on Titan. *Science* **222**, 119–120.
- McKay, C. P., Pollack, J. B. and Courtin, R. (1989) The thermal structure of Titan's atmosphere. *Icarus* **80**, 23–53.
- Morrison, D., Owen, T. and Soderblom, L. A. (1986) The satellites of Saturn. In *Satellites*, eds J. A. Burns and M. S. Matthews. University of Arizona Press, Tucson.
- Muhleman, D. O., Grossman, A. W., Butler, B. J. and Slade, M. A. (1991) Radar reflectivity of Titan. *Science* **248**, 975–980.
- Muhleman, D. O., Grossman, A. W. and Butler, B. J. (1995) Radar investigation of Mars, Mercury and Titan. *Ann. Rev. Earth Planet. Sci.* **23**, 337–374.
- Neff, J. S., Humm, D. C., Bergstrahl, J. T., Cochran, A. L., Cochran, W. C., Barker, E. S. and Tull, R. G. (1984) Absolute spectrophotometry of Titan, Uranus and Neptune: 3500–10500 Angstroms. *Icarus* **60**, 221–235.
- Noll, K. S. and Knacke, R. F. (1993) Titan: 1 to 5 micron photometry, spectrophotometry, and a search for variability. *Icarus* **101**, 272–281.
- Noll, K. S., Geballe, T. R., Knacke, R. F. and Pendleton, Y. J. (1996) Titan's 5-micron spectral window: carbon monoxide and the albedo of the surface. *Icarus* **124**, 625–631.
- Nozette, S., Lichtenberg, C. L., Spudis, P., Bonner, R., Ort, W., Malaret, E., Robinson, M. and Shoemaker, E. (1996) Clementine bistatic radar experiment: preliminary results. *Lunar and Planetary Science Conference (abstracts)*, Vol. 27, p. 967.
- Ostro, S. J. and Shoemaker, E. M. (1990) The extraordinary radar echoes from Europa, Ganymede and Callisto: a geological perspective. *Icarus* **85**, 335–345.
- Ostro, S. J. *et al.* (1992) Europa, Ganymede and Callisto: new radar results from Arecibo and Goldstone. *J. Geophys. Res.* **97**, 18,244–18,277.
- Pettengill, G. (1965) Lunar radar reflections. In *Solar System Radio Astronomy*, ed. J. Aarons, p. 355. Plenum Press, New York.
- Samuelson, R. E. and Mayo, L., Nath, N. (1996) Condensation and precipitation in Titan's atmosphere. *Bull. Am. Astron. Soc.* **28**, 1133.
- Sagan, C. and Dermott, S. F. (1982) The tides in the seas of Titan. *Nature* **300**, 731–733.
- Saint-Pe, O., Combes, M., Rigaut, F., Tomasko, M. and Fulchignoni, M. (1993) Demonstration of adaptive optics for resolved imagery of solar system objects: preliminary results on Pallas and Titan. *Icarus* **105**, 263–270.
- Schmitt, B., Quirico, E. and Lellouch, E. (1992) Near-infrared spectra of potential solids at the surface of Titan. *Symposium on Titan*, ESA SP-338, pp. 383–388.
- Sears, W. D. (1995) Tidal dissipation in oceans on Titan. *Icarus* **113**, 39–56.
- Smith, P. H., Lemmon, M. T., Lorenz, R. D., Sromovsky, L. A., Caldwell, J. J. and Allison, M. D. (1996) Titan's surface, revealed by HST imaging. *Icarus* **119**, 336–349.
- Sohl, F., Sears, W. D. and Lorenz, R. D. (1995) Tidal dissipation on Titan. *Icarus* **115**, 278–294.
- Stammes, P. (1992) The detectability of Titan's surface in the

- near-infrared. *Symposium on Titan*, ESA SP-338, pp. 205–210.
- Stevenson, D. J. (1992) The interior of Titan. *Symposium on Titan*, ESA SP-338, pp. 17–22.
- Stevenson, D. J. and Potter, B. E. (1986) Titan's latitudinal temperature distribution and seasonal cycle. *Geophys. Res. Lett.* **13**, 93–96.
- Yung, Y. L., Allen, M. and Pinto, J. P. (1984) Photochemistry of the atmosphere of Titan: comparison between model and observations. *Astrophys. J. (Suppl. Ser.)* **55**, 465–506.